

**Please cite the Published Version**

Bonacin, JA, Dos Santos, PL, Katic, V, Foster, CW and Banks, CE (2017) Use of Screen-printed Electrodes Modified by Prussian Blue and Analogues in Sensing of Cysteine. *Electroanalysis*, 30 (1). pp. 170-179. ISSN 1040-0397

**DOI:** <https://doi.org/10.1002/elan.201700628>

**Publisher:** Wiley

**Downloaded from:** <https://e-space.mmu.ac.uk/620838/>

**Additional Information:** "This is the peer reviewed version of the following article: Use of Screen-printed Electrodes Modified by Prussian Blue and Analogues in Sensing of Cysteine, which has been published in final form at 10.1002/elan.201700628. This article may be used for non-commercial purposes in accordance with Wiley Terms and Conditions for Use of Self-Archived Versions."

**Enquiries:**

If you have questions about this document, contact [openresearch@mmu.ac.uk](mailto:openresearch@mmu.ac.uk). Please include the URL of the record in e-space. If you believe that your, or a third party's rights have been compromised through this document please see our Take Down policy (available from <https://www.mmu.ac.uk/library/using-the-library/policies-and-guidelines>)

1 **Use of screen-printed electrodes modified by Prussian blue and analogues in sensing**  
2 **of cysteine**

3 Juliano A. Bonacin<sup>a\*</sup>, Vera Katic<sup>a</sup>, Pãmyla L. dos Santos<sup>a</sup>, Christopher W. Foster<sup>b</sup>, Craig E. Banks<sup>b\*</sup>

4 <sup>a</sup>Institute of Chemistry, University of Campinas, P. O. Box 6154, 13083-970, Campinas, SP, Brazil

5 Web: <http://bonacin.iqm.unicamp.br> Fax: +55 19 3521 3023; Tel: +55 19 3521 3103;

6 *e-mail*: \*jbonacin@iqm.unicamp.br

7 <sup>b</sup> Faculty of Science and Engineering, Manchester Metropolitan University, Chester Street, Manchester  
8 M15 GD, UK.

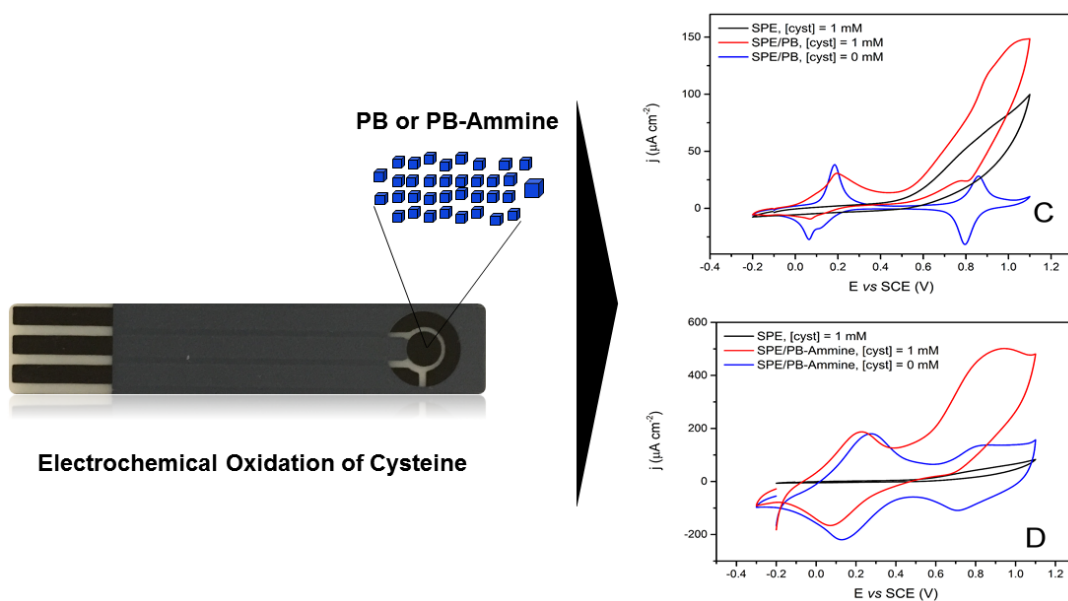
9 Web: <http://www.craigbanksresearch.com> Fax: +44 (0)1612476831; Tel: +44 (0)1612471196;

10 *e-mail*: \*c.banks@mmu.ac.uk

11

12 **Graphical Abstract**

13



14

15

16

17

18

19

1

2 **Abstract**

3       The utilisation of screen-printing technology allows for a mass scalable approach to producing  
4 electrochemical screen-printed electrodes (SPEs) and the presence of a redox mediator can add new  
5 possibilities to the electrochemical properties of the SPEs. Among the materials used as redox mediators,  
6 cyanidoferrates polymers can be used for electro-oxidation of cysteine. In this work, different monomers  
7  $[\text{Fe}(\text{CN})_6]^{4-}$  and  $[\text{Fe}(\text{CN})_5\text{NH}_3]^{3-}$  were used to produce Prussian blue (PB) and Prussian blue-Ammine  
8 (PB-Ammine), respectively. In addition, two modification methods were compared, the drop-casting  
9 and the incorporation of these materials into a *printable ink* were both used. The SPE modified by PB-  
10 Ammine (drop-casting) has the highest electroactive area and the highest heterogeneous rate constants  
11 are found in SPE modified by PB-Ammine incorporated into the ink. The highest value of the constant  
12 of electro-oxidation of cysteine and lowest limit of detection was observed in the SPE modified by PB  
13 incorporated into the ink. The studies suggest that the electrocatalytic properties of SPE modified by PB  
14 and PB-Ammine are dependents of the availability of  $\text{Fe}^{3+}$  catalytic sites and the faster chemical reaction  
15 between the catalytic sites and the analyte.

16

17

18

19       **Keywords:** screen-printed electrodes; Prussian blue; Prussian blue-Ammine, cysteine;  
20 electrocatalysis;

## 1 **1. Introduction**

2 The development of screen-printed electrodes (SPEs) has become a revolution in the world of  
3 electrochemical sensors<sup>[1,2]</sup>. SPEs are planar devices, based upon multiple layers of printable inks that  
4 simplify the electroanalytical procedure. Such electrodes allow laboratory analyses to be performed on-  
5 site and are suitable for working with microvolumes and decentralized assays <sup>[3-5]</sup>. Furthermore, the  
6 ability to mass produce these screen-printed electrodes reproducibly allows their use as one-shot sensors,  
7 alleviating potential memory effects and contamination whilst eradicating the requirement of electrode  
8 pretreatment and preparation (electrode polishing, potential cycling *etc.*), as is often the case for  
9 conventional solid electrodes (such as glassy carbon, boron-doped diamond and *etc.*)<sup>[6-8]</sup>.

10 SPEs have been widely used in clinical, environmental, biological, food safety and industrial  
11 analysis. The variety of commercial SPEs are available with an array of characteristics (*i.e.* different  
12 inks, substrates and heat curing temperatures) that directly influence on their electrochemical  
13 behavior<sup>[3,5,6]</sup>. Typically, carbon materials used as the screen-printed mediators are widely applied within  
14 electrochemical research for the determination of biological analytes such as NADH, dopamine or  
15 cysteine. In this sense, the analysis of the level of cysteine in the blood may reveal its deficiency and  
16 consequently be associated with the slow growth of children, some types of edemas, skin lesions,  
17 lethargy, liver damage, diabetes and mainly leukemia, Alzheimer and Parkinson's diseases<sup>[9,10]</sup>.

18 The electroactive layer is the key to the transduction process in the electrochemical sensing of  
19 molecular targets. Due to this, the electroactive coordination polymers (ECP) prepared from  
20 cyanidoferrates(II) deserve attention owing to the well-defined chemical behavior, stability of the film,  
21 facility in the preparation and wide range of application. In addition, the modulation of the  
22 electrochemical processes can be easily achieved by the strategic replacement of ligands in the complex  
23 and consequently, the properties are transferred to the ECP<sup>[11,12]</sup>.

24 Prussian blue is a classic example of an ECP that can have its electrochemical behavior  
25 modulated according to the starting complex. For example, ECP or Prussian blue analogous (Prussian

1 blue-Ammine) produced from  $[\text{Fe}(\text{CN})_5(\text{NH}_3)]^{3-}$  have a shift of the electrochemical process  $\text{Fe}^{2+}/\text{Fe}^{3+}$  to  
2  $\text{Fe}^{3+}/\text{Fe}^{3+}$  to lower value when compared with the same process in the Prussian blue. The shift observed  
3 is caused by lowering of energy levels of the HOMO orbital of the complex that is influenced by the  
4 sigma-donor character of  $\text{NH}_3$  as ligand in the iron complex<sup>[12,13]</sup>. This modulation can be essential for  
5 the design of new types of sensors.

6 In this paper, we report the electrochemical behavior of a SPE modified with Prussian blue and  
7 Prussian blue-Ammine produced from  $[\text{Fe}(\text{CN})_5\text{NH}_3]^{3-}$  towards the sensing of cysteine. In addition, we  
8 compare the characteristics of SPEs with the electroactive materials incorporated within the ink and  
9 drop-cast upon the electrode.

## 10 **2. Experimental**

### 11 *2.1. Chemicals*

12 Sodium nitroprusside ( $\text{Na}_2[\text{Fe}(\text{CN})_5\text{NO}]\cdot 2\text{H}_2\text{O}$ ) was purchased from Acros Organics. Iron(III)  
13 chloride, hydrochloric acid (HCl, 36.5-38%), potassium chloride (KCl), acetic acid ( $\text{CH}_3\text{CO}_2\text{H}$ , 99.7%)  
14 and sodium acetate ( $\text{CH}_3\text{CO}_2\text{Na}$ ) were purchased from Synth. Sodium iodide (NaI) and ethanol  
15 ( $\text{CH}_3\text{CH}_2\text{OH}$ ) were purchase from Merck. Ammonium hydroxide ( $\text{NH}_4\text{OH}$ , 28% m/v) and L-cysteine  
16 hydrochloride ( $\text{HSCH}_2\text{CH}(\text{NH}_2)\text{COOH}\cdot\text{HCl}$ ) were purchased from Sigma-Aldrich. All chemicals were  
17 of analytical grade and used without any further purification and the aqueous solutions were prepared  
18 with ultrapure water ( $>18\text{M}\Omega\text{ cm}$ ) obtained from a Milli-Q Plus system (Millipore).

### 19 *2.2. Synthesis of $\text{Na}_3[\text{Fe}(\text{CN})_5\text{NH}_3]\cdot 3\text{H}_2\text{O}$*

20 Sodium amminepentacyanidoferrate(II) was prepared by addition of 6.0 g of sodium nitroprusside  
21 in 40 mL of ammonium hydroxide in an Erlenmeyer. The mixture was stirred until the complete  
22 solubilization of  $\text{Na}_2[\text{Fe}(\text{CN})_5\text{NO}]\cdot 2\text{H}_2\text{O}$ . The Erlenmeyer was covered with aluminium foil and the top  
23 of the flask covered with cotton to allow the gas to exit. The solution was kept at room temperature,  
24 without stirring and in the dark for 3h, turning into dark yellow. Then, 6.0 g of NaI was added for

1 precipitation of a yellow solid. Finally, ethanol was slowly added to complete precipitation of the solid.  
2 The final product was filtered, washed with ethanol and dried under vacuum until constant weight. Yield:  
3 87%. Elemental analysis calculated for  $C_5H_9FeN_6Na_3O_3$  ( $325.98 \text{ g mol}^{-1}$ ): C 18.42%, H 2.78%, N  
4 25.78%. Found: C 18.51%, H 2.69% and N 25.37%.

### 5 *2.3.Synthesis of the ferric cyanidoferrates polymers*

6 Ferric hexacyanidoferrate(II), known as Prussian blue (PB) and ferric pentacyanidoferrate(II) (PB-  
7 Ammine) were prepared by chemical method. It consists in adding  $FeCl_3$  in excess ( $4.10^{-2} \text{ mol L}^{-1}$ ) to a  
8 solution of potassium hexacyanidoferrate or sodium amminepentacyanidoferrate ( $1.10^{-2} \text{ mol L}^{-1}$ ) under  
9 stirring. After 15 minutes, PB or PB-Ammine was precipitated in acetone and it was isolated by  
10 centrifugation.

### 11 *2.4.Modification of the electrodes*

12 The bare screen-printed electrodes (SPEs) were fabricated as described previously<sup>[14,15]</sup>. The  
13 modified SPEs by ECP were prepared by two different methods. Firstly,  $5.0 \mu\text{L}$  of suspensions of PB  
14 ( $2.0 \text{ mg mL}^{-1}$ ) and PB-Ammine ( $2.0 \text{ mg mL}^{-1}$ ) were drop-casted upon the surfaces of SPEs, which were  
15 subsequently left to dry overnight under vacuum at room temperature. The modified electrodes produced  
16 by the drop-casting method were labeled SPE/PB and SPE/PB-Ammine. Secondly, 10% (m/m) of PB  
17 and PB-Ammine were incorporated into the carbon-graphite ink (product code C2000802P2; Gwent  
18 Electronic Materials Ltd., U.K.) and used in the same printing process of the bare SPEs. The modified  
19 SPEs fabricated *via* the second method were labeled PB-SPE and PB-Ammine-SPE. After the  
20 modification, the SPEs were activated by applying 25 voltammetric cycles from  $-0.2 \text{ V}$  to  $0.6 \text{ V}$  vs SCE  
21 in a solution of  $HCl$   $0.1 \text{ mol L}^{-1}$  containing  $KCl$   $0.1 \text{ mol L}^{-1}$  at a scan rate of  $50 \text{ mV s}^{-1}$ . Afterwards, the  
22 electrodes were dried in an oven at  $60^\circ\text{C}$  for 1 hour.

## 1 2.5. Electrochemical measurements

2 Cyclic voltammetry (CV) measurements of SPE/PB and SPE/PB-Ammine were carried out using  
3 a Palmsens Emstat (Palmsens, Netherlands) potentiostat. CV of PB-SPE and PB-Ammine-SPE were  
4 performed on an AUTOLAB modular electrochemical system (ECO Chemie, Utrecht, Netherlands)  
5 equipped with a STAT 12 module and driven by NOVA 2.1 software. The bare or modified SPE were  
6 used as working electrode, a saturated calomel electrode (SCE) as reference electrode, and a platinum  
7 wire as auxiliary electrode. Acetate buffer (ABS, pH=6) containing KCl and HCl/KCl (pH=1) solutions  
8 were used for the stability measurements. Oxygen was removed by bubbling nitrogen for approximately  
9 10 min through the solution before each electrochemical measurement.

10 The electroactive areas of the SPEs were determined *via* cyclic voltammetry in 1.0 mmol L<sup>-1</sup> of  
11 [Ru(NH<sub>3</sub>)<sub>6</sub>]<sup>3+</sup> and 0.1 mol L<sup>-1</sup> KCl at different scan rates, according to the Randles-Ševčíck equation  
12 (Eq.1):

$$13 \quad i_p = 2.69 \times 10^5 n^{\frac{3}{2}} A D^{\frac{1}{2}} C v^{\frac{1}{2}} \quad (1)$$

14 The heterogeneous rate constants of the SPEs,  $k^0$ , were presented determined using the Nicholson  
15 method by the following equation (Eq.2):

$$16 \quad k^0 = \left[ 2.18 \left( \frac{D \alpha n F v}{RT} \right)^{\frac{1}{2}} \right] \exp \left[ - \left( \frac{\alpha^2 n F}{RT} \right) \Delta E_p \right] \quad (2)$$

17 were  $i_p$  is the peak current,  $n$  is the number of electrons transferred in the electrochemical process,  $A$  is  
18 electrode area,  $D$  is the diffusion coefficient ( $9.10 \times 10^{-6} \text{ cm}^2 \text{ s}^{-1}$  for [Ru(NH<sub>3</sub>)<sub>6</sub>]<sup>3+</sup>),  $C$  is the redox probe  
19 concentration and  $v$  is the applied voltammetric scan rate,  $R$  the gas constant, and  $T$  the temperature of  
20 the solution,  $\alpha$  is assumed to correspond to 0.5,  $\Delta E_p$  is peak-to-peak separation<sup>[4,16]</sup>.

## 1 2.6. Cysteine detection

2 Electrochemical detection of cysteine was carried out in the same conventional three-electrode  
3 electrochemical cell. Chronoamperometry measurements were performed at applied potential of 0.8 V  
4 vs. SCE, upon successive additions of 0.1 mol L<sup>-1</sup> L-cysteine hydrochloride stock solution, under N<sub>2</sub>  
5 atmosphere. Acetate buffer solution (0.1M, pH=6.0) containing 0.1 M KCl was used as supporting  
6 electrolyte.

7

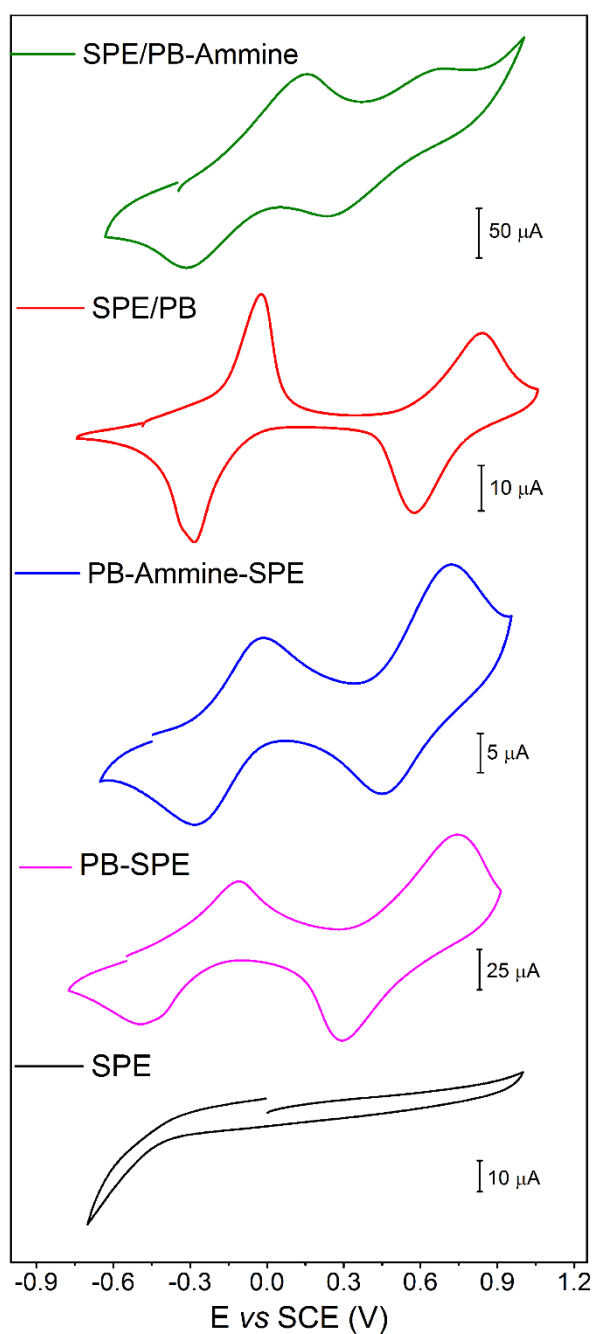
## 8 3. Results and Discussion

### 9 3.1. Electrochemical properties of the screen-printed electrodes

15 The electrochemical behavior of the bare and modified SPEs was investigated by cyclic  
16 voltammetry and is depicted within Figure 1. The bare SPE does not exhibit any redox peaks. After 30  
17 voltammetric cycles (Fig. S1), the capacitive current increases, probably due to the alterations in the  
18 surface area and roughness of the electrodes. Functional groups, impurities, defects and edge plane-like  
19 sites on the graphite present in the ink also contribute to alterations within the double-layer  
20 capacitance<sup>[17,18]</sup>.

21





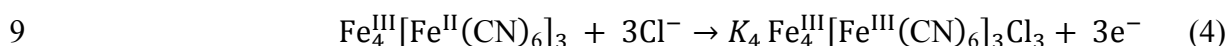
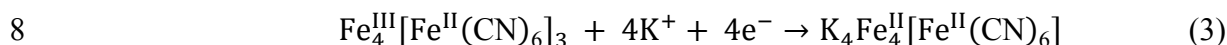
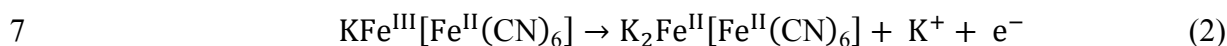
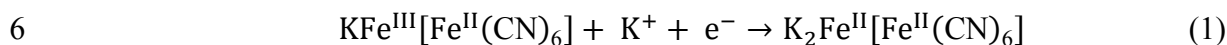
1

2 **Figure 1:** Comparison between the cyclic voltammograms of the bare SPE and modified: PB-SPE, PB-  
 3 Ammine-SPE, SPE/PB and SPE/PB-Ammine in 0.1 M ABS (pH = 6.0) and 0.1 M KCl at 50 mV s<sup>-1</sup>.

4

5 All the modified SPEs exhibit two well-defined pairs of redox peaks ~ + 0.12 and + 0.80 V vs.  
 6 SCE, which are ascribed to the electrochemical process between Prussian white (PW) to PB (Fe<sup>2+</sup>/Fe<sup>2+</sup>  
 7 → Fe<sup>2+</sup>/Fe<sup>3+</sup>), and PB to Belin green (BG, Fe<sup>2+</sup>/Fe<sup>3+</sup> → Fe<sup>3+</sup>/Fe<sup>3+</sup>), respectively. The composition of the

1 modified SPEs is associated with the “insoluble” form of the ferric cyanidoferrate, synthesized from  
2 excess of Fe<sup>3+</sup>. The “insoluble” form can be converted to the “soluble” after performing cyclic  
3 voltammetry experiments in KCl, because of the insertion of K<sup>+</sup> in the interstitial sites of the PB<sup>[19]</sup>. The  
4 reduction and oxidation reactions of “soluble” (Eq. 1 and 2) and “insoluble” forms of PB (Eq. 3 and 4)  
5 as described as follow<sup>[20]</sup>:



10 As described by the Eq. 1-4, the electrochemical process of Prussian blue is mediated by the  
11 transport of K<sup>+</sup> and Cl<sup>-</sup> into and out of the film to maintain the electroneutrality. Thus, the redox processes  
12 of the modified electrodes are not surface-confined and depend on the diffusion of the ions into the  
13 structure of the materials. This is confirmed by the non-linear correlation between the peak current and  
14 the scan rates, as presented in Figures S.2-S.5.

15 The formal potential values of these processes ( $E_{1/2}$ ) at the modified electrodes are presented in  
16 Tables S7-S8. The lowest values of  $E_{1/2}$  of the SPE modified with PB-Ammine reflects the weaker  $\pi$ -  
17 acceptance character of the NH<sub>3</sub> ligand when compared with CN<sup>-</sup>, consequently Fe<sup>3+</sup> has a higher charge  
18 density facilitating the oxidation of this metal<sup>[13]</sup>.

19 To study the electron transfer properties and determine the electroactive areas ( $A_e$ ) of the bare  
20 and modified SPEs, cyclic voltammetry was carried out in the presence of the outer-sphere redox probe  
21 hexaammineruthenium(III) in 0.1 M KCl, Figure S.6.

1 The electroactive areas of the PB or electroactive coordination polymers can be modulated by  
 2 the utilisation of different monomers. Recently, an improvement of the  $A_e$  of the PB produced from  
 3 pentacyanidoferrate complexes by drop-casting and potentiostatic methods was reported<sup>[11,12,21]</sup>. PB  
 4 polymers with fcc structures are produced from hexacyanidoferrates complexes. The substitution of one  
 5  $CN^-$  to N-heterocycles ligands as isn (pyridine-4-carboxylate)<sup>[21]</sup>, mpz (N-methylpyrazinium)<sup>[12]</sup> and ppt  
 6 (5-(4-pyridil)-1H-1,2,4-triazole-3-thiol)<sup>[11]</sup> promotes loss of symmetry and crystallinity of the polymers.  
 7 Thus, the higher electroactive area of SPE/PB-Ammine produced can be associated to its structural  
 8 defects. On the contrary, the PB-Ammine-SPE presents the lower electroactive area, due to its decreased  
 9 dispersibility in the carbonaceous matrix compared to the PB-SPE.

10 According to Table 1, the modified electrodes produced by the drop-casting method present  
 11 larger electroactive areas, because of higher amount of the PB and PB-Ammine utilized and it reflects  
 12 in the heterogeneous rate constants ( $k^0$ ). The increase of the peak-to-peak separation in the  
 13 voltammograms (Table S.9) indicates the slower electron transfer after the modification of the  
 14 electrodes. The ferric cyanidoferrates polymers have partially blocked the interfacial charge transfer of  
 15 the redox probe. The faster heterogenous electron transfer from the redox probe to the PB-Ammine-SPE  
 16 is also attributed to the low dispersibility of this material and better exposure of the conductive carbon  
 17 material used in the ink.

18 **Table 1:** Electroactive areas and heterogeneous rate constants of the SPEs

Electrode	Method	$A_e$ (cm <sup>2</sup> )	$k^0$ (cm s <sup>-1</sup> )
SPE		0.0718	1.91 x 10 <sup>-3</sup>
PB-SPE	ink*	0.0892	1.00 x 10 <sup>-3</sup>
PB-SPE-Ammine	ink*	0.0466	1.28 x 10 <sup>-3</sup>
SPE/PB	drop-casting	0.0829	1.02 x 10 <sup>-3</sup>
SPE/PB-Ammine	drop-casting	0.0992	0.23 x 10 <sup>-3</sup>

19 \*incorporation of ECP into the ink

### 3.2. Stabilities of the modified screen-printed electrodes at different pH

The stabilities of the modified electrodes were investigated by cyclic voltammetry in 0.1 M ABS (pH 6.0) containing 0.1 M KCl and in 0.1 M HCl/KCl (pH 1.0), according to Figures S.7-10. The percentages of PB or PB-Ammine film in function of the scan is showed in Figure 2. The lower stability of the modified SPEs at pH 6.0 compared to pH 1.0 was as expected, due to the affinity of OH<sup>-</sup> ions for Fe(III) at pH close to 7.0, breaking the Fe<sup>2+</sup>-(CN)-Fe<sup>3+</sup> bond [22].

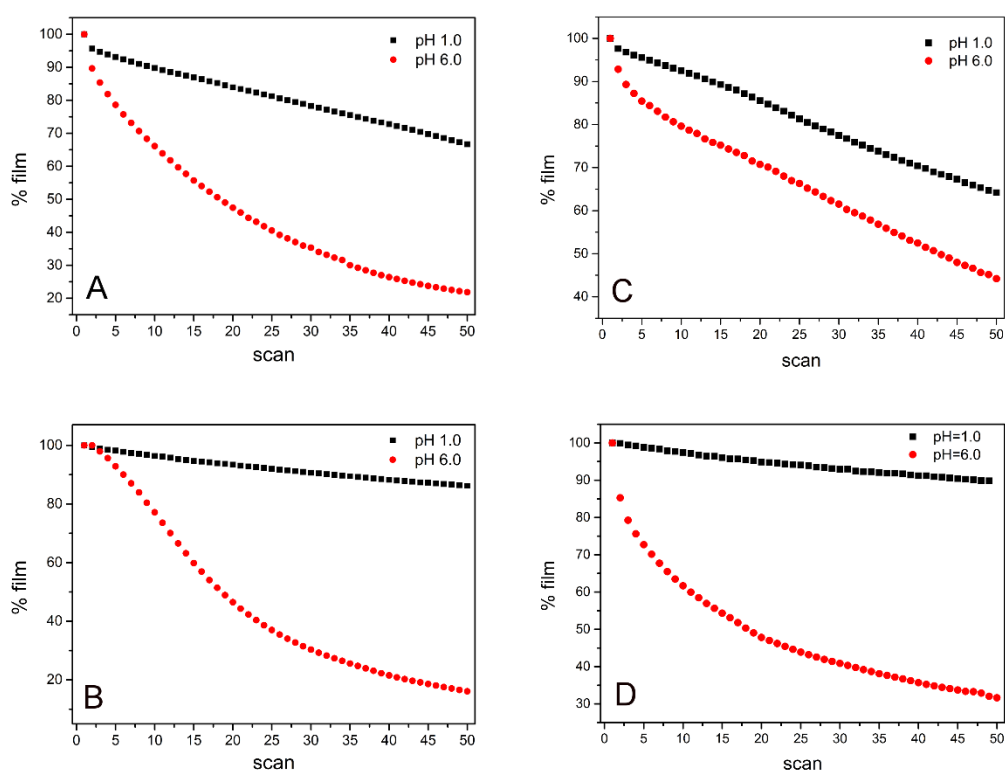


**Figure 2:** Comparison between the percentages of films in function of the number of scans at pH 1.0 and 6.0 of the modified electrodes: *incorporation of ECP into the ink:* **A)** PB-SPE, **B)** PB-Ammine-SPE, *drop-casting:* **C)** SPE/PB and **D)** SPE/PB-Ammine.

It is well known that the stability of the ferric hexacyanidoferrates polymers can be increased by electrochemical and thermal activations. These processes decrease the structural defects caused by the coordination of OH<sup>-</sup> to Fe<sup>3+</sup> during the formation of PB or PB-Ammine and remove water present within the crystals. However, the lability of the NH<sub>3</sub> ligand favours the exchange to H<sub>2</sub>O or OH<sup>-</sup> [23] at pH 6.0, affecting the structure of the SPEs modified with PB-Ammine and explains their lower stabilities.

1 The stability of the ferric cyanidoferrates polymers is also dependent on the method of deposition,  
2 due to the difference in availability of the ferric ions which can react with OH<sup>-</sup>. In addition, the “soluble”  
3 form of PB is reported as the most stable one. From electrochemical activation, the “insoluble” form of  
4 Prussian can be converted in to “soluble” form by insertion of K<sup>+</sup> in the interstitial sites<sup>[24]</sup>. However,  
5 only the superficial layers of PB are able to be converted, due to direct contact with the KCl solution<sup>[19]</sup>.  
6 It can explain the higher stability and more effective activation of the modified SPEs by drop-casting  
7 than the modification with the ink. In the other method, PB and PB-Ammine crystals are in the bulk of  
8 the electrode, entrapped in the carbonaceous matrix, presented as “insoluble” form.

9

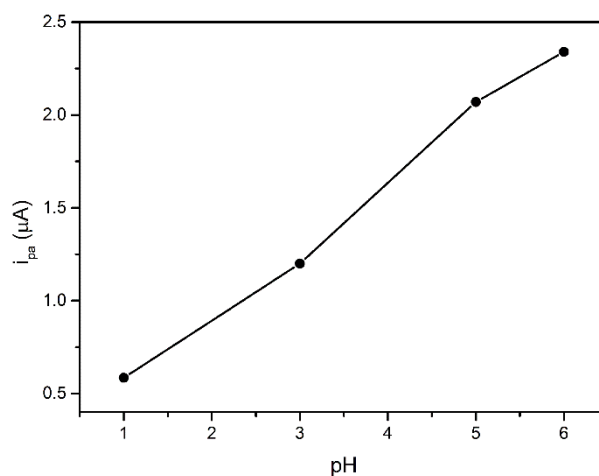
### 10 3.3. *Electrocatalytic properties*

11 To determine the effect of pH on the electro-oxidation of cysteine at the bare SPE, cyclic  
12 voltammetry experiments at different pH in the presence of the analyte were performed (Figure S.11).  
13 The electrochemical oxidation of cysteine (RSH) to disulfide cystine (RSSR) on the bare SPE surface  
14 is proceed by Eq.5-7:



18 As it can be seen in Figure 3, the peak current increases with the pH. At higher pH deprotonation  
19 of RSH (pKa = 8.37) occurs producing RS<sup>-</sup>, which is oxidized to RSSR *via* formation of sulfide  
20 radical<sup>[25]</sup>, explaining the better response at pH 6.0. The lower peak potential at pH 6.0 is also explained  
21 as function of the deprotonation of cysteine. According to Fei and co-authors, at alkaline medium, the  
22 oxidation peak shifts to more cathodic potentials<sup>[26]</sup>. However, detection of cysteine in alkaline solution  
23 affects the stability of the ferric cyanidoferrates polymers. In our previous report, it was demonstrated  
24 that acetate buffer solution is the best choice for electrochemical experiments using modified electrodes

1 with PB and analogues coordination polymers, causing small alterations in its structure<sup>[12]</sup>. In this sense,  
2 pH 6.0 is more appropriate for cysteine detection.

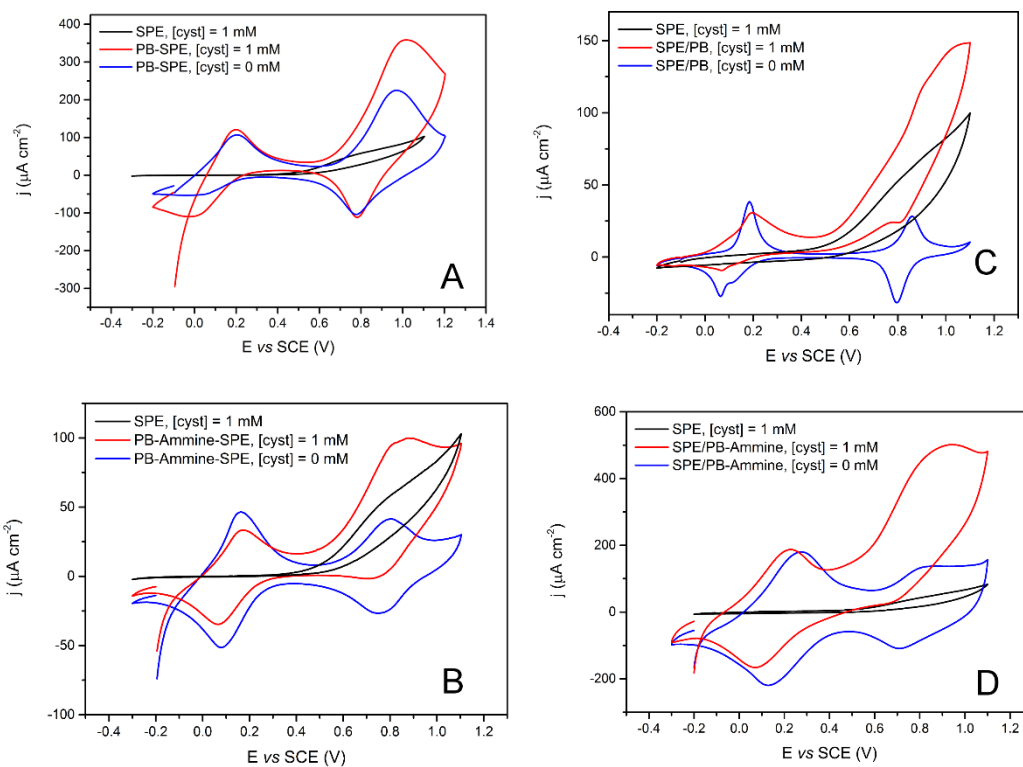


3

4 **Figure 3:** Plot of peak current of cysteine electro-oxidation at the bare SPE *versus* pH, in 1 mM cysteine  
5 and 0.1 M KCl/HCl (pH 1.0) or 0.1 M ABS/KCl (pH 3.0, 5.0 and 6.0), at  $5 \text{ mV s}^{-1}$ .

6

7 The electro-oxidation of cysteine at the bare and modified SPEs was compared by cyclic  
8 voltammetry at the chosen pH. Upon addition of cysteine, a pronounced increase of the current density  
9 was observed for the modified SPEs, due to the electrocatalytic activity of the PB and PB-Ammine  
10 toward the oxidation of the analyte, Figure 4 .

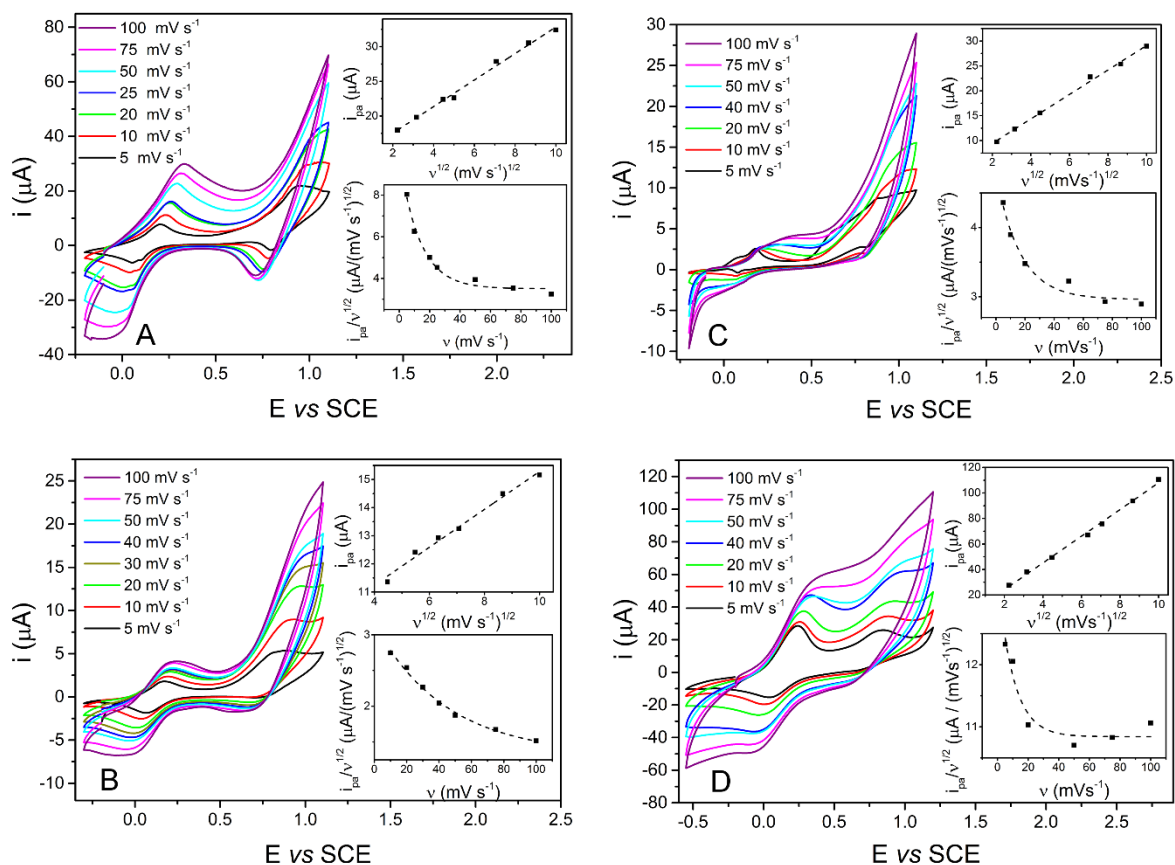


1

2 **Figure 4:** Comparison between the cyclic voltammograms of the bare SPE and modified: **A)** PB-SPE,  
 3 **B)** PB-Amphine-SPE, **C)** SPE/PB and **D)** SPE/PB-Amphine in the absence and presence of 1 mM of  
 4 cysteine. All the measurements were performed in 0.1 M ABS (pH = 6.0) and 0.1 M KCl at  $5 \text{ mV s}^{-1}$ .

5

6 For better understanding of the electro-catalytic oxidation of cysteine on the surface of the  
 7 modified SPEs, cyclic voltammetry experiments at different scan rates in presence of 1.0 mM of this  
 8 analyte were performed, Figure 5.



1

2 **Figure 5:** Cyclic voltammograms of **A)** PB-SPE, **B)** PB-Ammin-SPE, **C)** SPE/PB and **D)** SPE/PB-  
 3 Ammin in presence of 1.0 mmol L<sup>-1</sup> at various scan rates. All studies were performed in 0.1 M ABS  
 4 (pH = 6.0) and 0.1 M KCl. Insert: plot of  $i_{pa}$  versus  $v^{1/2}$  and plot of  $i_{pa}/v^{1/2}$  versus  $v$ .

5

6 The catalytic oxidation peak current ( $i_{pa}$ ) increases linearly in function of the square of the  
 7 scan rate ( $v^{1/2}$ ) in all modified electrodes, indicating that the electro-catalytic processes are controlled by  
 8 diffusion of cysteine at the studied scan rate range in all modified electrodes, as can be expressed by Eq.  
 9 8-11 for the PB-SPE (ink), PB-Ammin-SPE (ink), SPE/PB (drop-casting) and SPE/PB-Ammin (drop-  
 10 casting), respectively. In addition, characteristic shapes of a catalytic electrochemical process ( $EC_{cat}$ )  
 11 were observed by plotting the scan rate normalized current ( $i_{pa}/v^{1/2}$ ) versus scan rate, confirming the  
 12 electro-catalytic efficiency of the ferric cyanidoferrate polymers.

13 
$$I(\mu A) = 13.7 + 1.9 v^{1/2}(mV s^{-1})^{1/2} \quad (8)$$

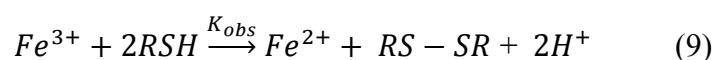
14 
$$I(\mu A) = 8.5 + 0.7 v^{1/2}(mV s^{-1})^{1/2} \quad (9)$$



$$I(\mu A) = 4.5 + 2.5 v^{\frac{1}{2}}(mV s^{-1})^{\frac{1}{2}} \quad (10)$$

$$I(\mu A) = 3.2 + 10.5 v^{\frac{1}{2}}(mV s^{-1})^{\frac{1}{2}} \quad (11)$$

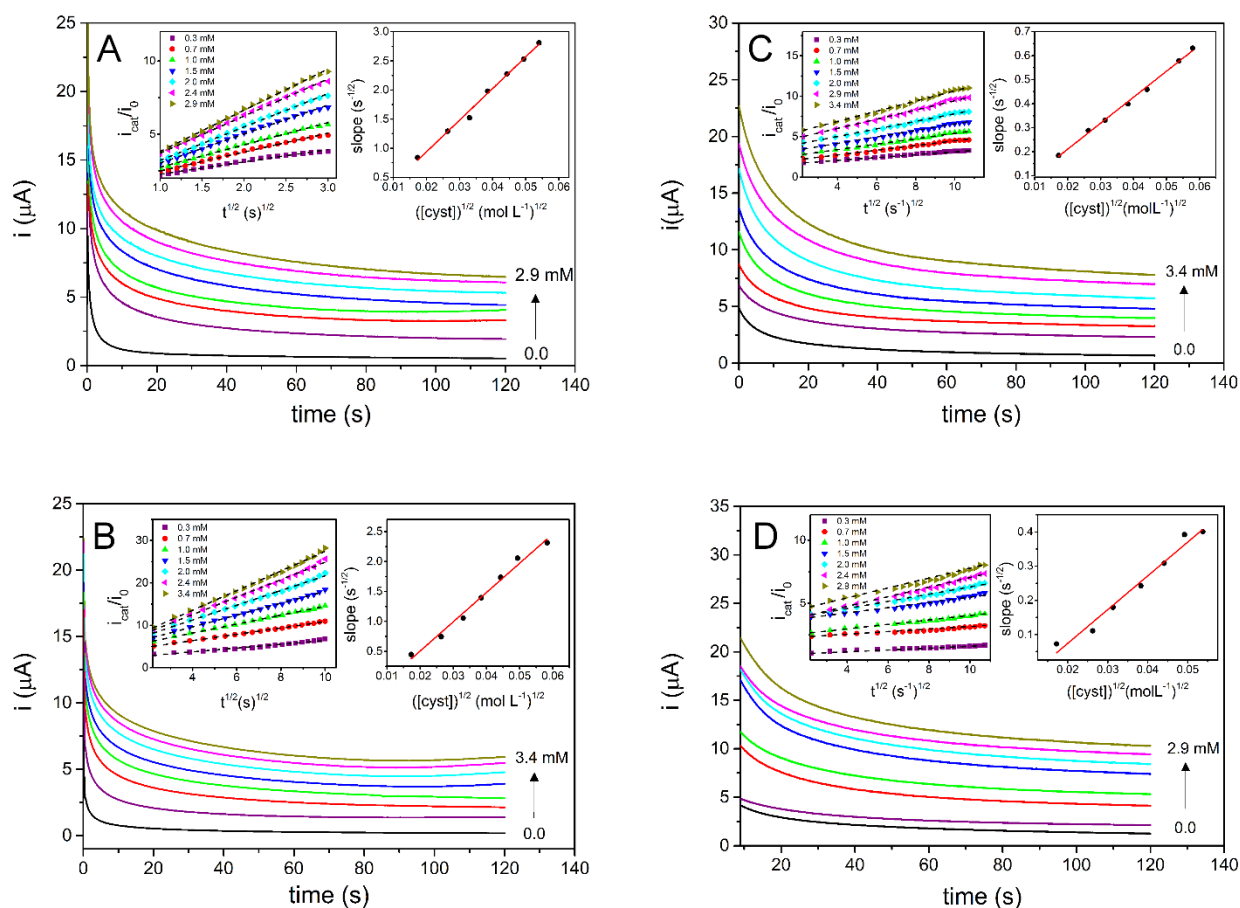
Cysteine (RSH) can be electro-oxidized to disulfide cysteine (RS-SR) by  $Fe^{3+}$  ions in the PB or PB-Ammine structures, which is reduced to  $Fe^{2+}$ . The generic reaction for cysteine oxidation on the surfaces of the modified SPEs has been proposed as follows:<sup>[27,28]</sup>



To compare the kinetic of the chemical reactions between the  $Fe^{3+}$  ions in the PB or PB-Ammine modified SPEs and cysteine, chronoamperometric experiments in the presence of different concentrations of the analyte were performed, Figure 6. The heterogeneous rate constants,  $k_{obs}$  of these reactions were determined according to Eq. 10.

$$\frac{i_{cat}}{i_0} = \gamma^{\frac{1}{2}} \pi^{\frac{1}{2}} = \pi^{\frac{1}{2}}(k_{obs}Ct)^{\frac{1}{2}} \quad (10)$$

where  $i_{cat}$  is the catalytic current of the modified SPEs in the presence of cysteine,  $i_0$  is the limiting current in the absence of cysteine and  $\gamma = k_{obs}Ct$  ( $C$  is the bulk concentration of cysteine and  $t$  is the elapsed time)<sup>[29]</sup>.



1

2 **Figure 6:** Chronoamperograms of **A)** PB-SPE, **B)** PB-Amphine-SPE, **C)** SPE/PB and **D)** SPE/PB-  
 3 Amphine in 0.1 M ABS at pH 6.0 different concentrations of cysteine. Inserts: Curves of  $i_{cat}/i_0$  versus  $t$   
 4  $^{1/2}$  for the same concentrations of cysteine, and plot of the slopes of these curves versus the square root  
 5 of the concentrations of cysteine.

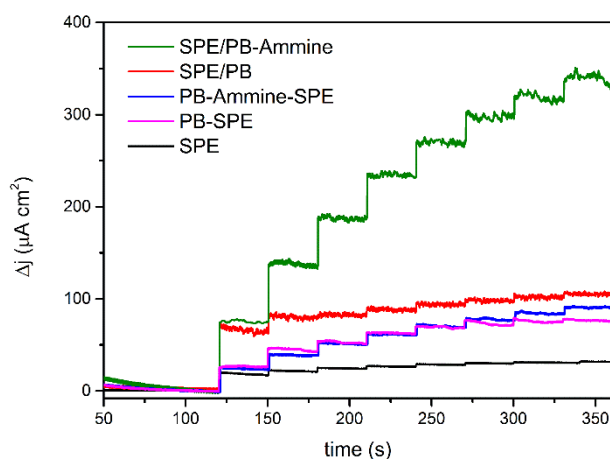
6

7 The heterogeneous rate constants were obtained from the linear plots of  $i_{cat}/i_0$  versus  $t^{1/2}$ . Then,  
 8 graphs of the slopes of these curves were plotted as a function of the square root of the concentrations  
 9 of cysteine ( $[\text{cyst}]^{1/2}$ ). Finally,  $k_{obs}$  were calculated from the slopes of these graphs, resulting in values  
 10 of  $9.4 \times 10^2$ ,  $3.6 \times 10^2$ ,  $3.7 \times 10^1$  and  $3.1 \times 10^1$  L mol $^{-1}$  s $^{-1}$  for PB-SPE (ink), PB-Amphine-SPE(ink), SPE/PB  
 11 (drop-casting) and SPE/PB-Amphine (drop-casting), respectively. The modified SPEs by the  
 12 incorporation of the materials in the ink presents lower stability due to more exposure of the Fe $^{3+}$ .  
 13 However, the high availability of these sites increases the heterogeneous rate constants for cysteine  
 14 electro-oxidation at PB-SPE and SPE-PB-Amphine. The faster kinetics of the chemical reactions

1 between the Fe<sup>3+</sup> ions in the PB-SPE and cysteine is attributed to the better distribution of this material  
 2 and its higher electroactive area. To compare the performances of the modified electrodes for sensing of  
 3 cysteine, chronoamperometric experiments were carried out.

#### 4 3.4. Chronoamperometric detection of cysteine

5 Aiming cysteine detection, Figure 7 displays the chronoamperometric responses of bare SPE,  
 6 SPE/PB (drop-casting), SPE/PB-Ammine (drop-casting), PB-SPE (ink) and PB-SPE-Ammine (ink)  
 7 after successive additions of cysteine in 0.1 mol L<sup>-1</sup> ABS and 0.1 mol L<sup>-1</sup> KCl at pH 6.0. As it can be  
 8 seen in Figure S.12, with an applied potential of 0.8 V vs SCE, the SPEs showed linear responses in the  
 9 ranges presented in Table 2.



10

11 **Figure 7:** Chronoamperograms of the bare and modified SPEs: PB-SPE, PB-Ammine-SPE, SPE/PB and  
 12 SPE/PB-Ammine in 0.1 M ABS at pH 6.0 and 0.1 M KCl after successive additions of 0.1 mol L<sup>-1</sup>  
 13 cysteine. Applied potential of 0.8 V vs SCE.

14 **Table 2:** Comparison of the amperometric responses of the modified electrodes

Electrode	Linear dependence	R <sup>2</sup>	Linear range	LOD
*PB-SPE	$\Delta i(\mu A) = 7.03 \times 10^{-3} [\text{cyst}](\mu M) + 2.80$	0.99	200-600 $\mu M$	45.1 $\mu M$
*PB-Ammine-SPE	$\Delta i(\mu A) = 3.61 \times 10^{-3} [\text{cyst}](\mu M) + 1.58$	0.99	300-800 $\mu M$	102.4 $\mu M$
†SPE/PB	$\Delta i(\mu A) = 4.24 \times 10^{-3} [\text{cyst}](\mu M) + 5.55$	0.99	300-700 $\mu M$	70.2 $\mu M$
†SPE/PB-Ammine	$\Delta i(\mu A) = 4.89 \times 10^{-2} [\text{cyst}](\mu M) + 3.58$	0.99	100-500 $\mu M$	58.6 $\mu M$

15 \*incorporation of ECP into the ink; †drop-casting

1           The electro-oxidation of cysteine at the surface of the modified SPEs begins with the  
2 deprotonation of this molecule, which is diffused from the bulk solution to the electrode surface. On the  
3 PB or PB-Ammine modified SPE surface, the deprotonated cysteine is oxidized by the  $\text{Fe}^{3+}$  ions in the  
4 PB or PB-Ammine in an electro-catalytic process. The performances of the electrodes towards detection  
5 of cysteine are dependent on the stabilities of the electrodes, the electron transfer from the modified  
6 electrode to the analyte, the availability of the ferric ions and the kinetics of the chemical reaction  
7 between the catalytic sites and the analyte. Comparing the different ferric cyanidoferrates and the  
8 modification methods, the lower detection limit was obtained at the PB-SPE, due to its high electroactive  
9 area and availability of  $\text{Fe}^{3+}$  catalytic sites. In addition, the incorporation of a non-conductive material  
10 as PB in the ink allows a less pronounced decrease of the heterogeneous electron transfer rate than the  
11 drop-casting method. Although PB-ammine electrochemical potentials are shifted to lower values than  
12 PB, the PB-ammine transfer rate is lower than PB (see Figure S.13). This feature can explain the  
13 differences observed in the oxidation of cysteine ( $k_{\text{obs}}$ ) and in the sensing of this analyte.

14

#### 15 **4. Conclusion**

16           Ferric cyanidoferrates polymers, PB and PB-Ammine, synthesized from different monomers  
17  $[\text{Fe}(\text{CN})_6]^{4-}$  and  $[\text{Fe}(\text{CN})_5\text{NH}_3]^{3-}$  were used to modify screen-printed electrodes. The modification was  
18 performed by two methods, the drop-casting and the incorporation of the materials in the ink used in the  
19 screen-printed process. The SPE modified by PB-Ammine (drop-casting) has the highest electroactive  
20 area. However, the highest heterogeneous rate constants are found in SPE modified by PB-Ammine  
21 incorporated into the ink. All of them have catalytic behaviour to electro-oxidation of cysteine, but the  
22 highest value of  $k_{\text{obs}}$  and lowest limit of detection was observed in the SPE modified by PB incorporated  
23 into the ink. These results suggest that the electrocatalytic properties of SPE modified by PB and PB-  
24 Ammine are dependents of the availability of  $\text{Fe}^{3+}$  catalytic sites and the faster chemical reaction between  
25 the catalytic sites and the analyte.

## 1 **Conflict of interest**

2 The authors declare that there is no conflict of interests regarding the publication of this study.

3

## 4 **Acknowledgements**

5 The authors acknowledge the financial support by CAPES, Fundo de Apoio ao Ensino, à  
6 Pesquisa e à Extensão - Universidade Estadual de Campinas, FAEPEX-UNICAMP (grant#2824/17),  
7 Conselho Nacional de Desenvolvimento Científico e Tecnológico (CNPq – grant#459923/2014-5) and  
8 Fundação de Amparo à Pesquisa do Estado de São Paulo (FAPESP - grant#2013/22127-2 and  
9 grant#2017/00461-9)

10

## 11 **Supporting Information**

12 Supporting Information associated with this article can be found in the online version.

13

## 14 **References**

- 15 [1] C. W. Foster, R. O. Kadara, C. E. Banks, in *Screen-Print. Electrochem. Archit.*, Springer  
16 International Publishing, Cham, **2016**, pp. 1–23.
- 17 [2] E. P. Randviir, D. A. C. Brownson, J. P. Metters, R. O. Kadara, C. E. Banks, *Phys. Chem. Chem.*  
18 *Phys.* **2014**, *16*, 4598.
- 19 [3] J. R. Windmiller, J. Wang, *Electroanalysis* **2013**, *25*, 29–46.
- 20 [4] F. E. Galdino, C. W. Foster, J. A. Bonacin, C. E. Banks, *Anal Methods* **2015**, *7*, 1208–1214.
- 21 [5] N. Jadon, R. Jain, S. Sharma, K. Singh, *Talanta* **2016**, *161*, 894–916.
- 22 [6] S. Sadeghi, A. Garmroodi, *Electroanalysis* **2013**, *25*, 323–330.
- 23 [7] C. W. Foster, J. P. Metters, D. K. Kampouris, C. E. Banks, *Electroanalysis* **2014**, *26*, 262–274.
- 24 [8] Y. Cui, *IEEE Trans. Electron Devices* **2017**, *64*, 2467–2477.

- 1 [9] S. Shahrokhian, *Anal. Chem.* **2001**, *73*, 5972–5978.
- 2 [10] M. C. Gallo, B. M. Pires, K. C. F. Toledo, S. A. V. Jannuzzi, E. G. R. Arruda, A. L. B. Formiga, J.  
3 A. Bonacin, *Synth. Met.* **2014**, *198*, 335–339.
- 4 [11] B. M. Pires, F. E. Galdino, J. A. Bonacin, *Inorganica Chim. Acta* **2017**, *466*, 166–173.
- 5 [12] M. C. Monteiro, K. C. F. Toledo, B. M. Pires, R. Wick, J. A. Bonacin, *Eur. J. Inorg. Chem.* **2017**,  
6 DOI 10.1002/ejic.201601540.
- 7 [13] A. L. B. Formiga, S. Vancoillie, K. Pierloot, *Inorg. Chem.* **2013**, *52*, 10653–10663.
- 8 [14] E. Blanco, C. W. Foster, L. R. Cumba, D. R. do Carmo, C. E. Banks, *The Analyst* **2016**, *141*, 2783–  
9 2790.
- 10 [15] S. J. Rowley-Neale, G. C. Smith, C. E. Banks, *ACS Appl. Mater. Interfaces* **2017**, *9*, 22539–22548.
- 11 [16] I. Lavagnini, R. Antiochia, F. Magno, *Electroanalysis* **2004**, *16*, 505–506.
- 12 [17] J. P. Metters, R. O. Kadara, C. E. Banks, *The Analyst* **2011**, *136*, 1067.
- 13 [18] L. R. Cumba, C. W. Foster, D. A. C. Brownson, J. P. Smith, J. Iniesta, B. Thakur, D. R. do Carmo,  
14 C. E. Banks, *The Analyst* **2016**, *141*, 2791–2799.
- 15 [19] F. Ricci, G. Palleschi, *Biosens. Bioelectron.* **2005**, *21*, 389–407.
- 16 [20] K. Itaya, I. Uchida, V. D. Neff, *Acc. Chem. Res.* **1986**, *19*, 162–168.
- 17 [21] B. Morandi Pires, S. A. Venturinelli Jannuzzi, A. L. Barboza Formiga, J. Alves Bonacin, *Eur. J.*  
18 *Inorg. Chem.* **2014**, *2014*, 5812–N5819.
- 19 [22] A. Karyakin, *Electrochem. Commun.* **1999**, *1*, 78–82.
- 20 [23] N. Ghasdian, Y. Liu, R. McHale, J. He, Y. Miao, X. Wang, *J. Inorg. Organomet. Polym. Mater.*  
21 **2013**, *23*, 111–118.
- 22 [24] R. J. Mortimer, D. R. Rosseinsky, *J. Chem. Soc. Dalton Trans.* **1984**, 2059.
- 23 [25] W. T. Tan, A. M. Bond, S. W. Ngooi, E. B. Lim, J. K. Goh, *Anal. Chim. Acta* **2003**, *491*, 181–191.
- 24 [26] S. Fei, J. Chen, S. Yao, G. Deng, D. He, Y. Kuang, *Anal. Biochem.* **2005**, *339*, 29–35.
- 25 [27] C. C. Corrêa, S. A. V. Jannuzzi, M. Santhiago, R. A. Timm, A. L. B. Formiga, L. T. Kubota,  
26 *Electrochimica Acta* **2013**, *113*, 332–339.
- 27 [28] N. Hernández-Ibáñez, I. Sanjuán, M. Á. Montiel, C. W. Foster, C. E. Banks, J. Iniesta, *J.*  
28 *Electroanal. Chem.* **2016**, *780*, 303–310.
- 29 [29] J.-B. Raouf, R. Ojani, H. Beitollahi, *Electroanalysis* **2007**, *19*, 1822–1830.
- 30